Heavy Flavor Physics Results from CMS

M. Galanti[1]
for the CMS Collaboration

[1] *Department of Physics, University of Cyprus, P.O. Box 20537, 1678 Nicosia, Cyprus*

Summary. — In this article, we summarize some recent heavy flavor measurements performed by the CMS experiment. The inclusive b production cross section, the study of $\Lambda_b \to J/\psi\Lambda$ and of other exclusive B-hadron decays, and the analysis of prompt and non-prompt J/ψ and $\psi(2s)$ are reviewed.

PACS `13.85.Ni` – Inclusive production with identified hadrons.
PACS `13.85.Qk` – Inclusive production with identified leptons, photons, or other nonhadronic particles.
PACS `14.20.Mr` – Bottom baryons (|B| > 0).
PACS `14.40.Nd` – Bottom mesons (|B| > 0).
PACS `14.40.Pq` – Heavy quarkonia.

1. – Introduction

The analyses presented here were all performed with data collected by the CMS experiment at LHC [1] during 2010 and 2011. In these two years, LHC has delivered proton-proton collisions with a center-of-mass energy $\sqrt{s} = 7\,\text{TeV}$, and the luminosity collected by CMS has been $\sim 40\,\text{pb}^{-1}$ in 2010 and $\sim 5\,\text{fb}^{-1}$ in 2011.

The heavy-flavor program of CMS relies mainly on specialized di-muon triggers, and takes advantage of the excellent tracking and vertexing capabilities of the CMS detector. The di-muon triggers make use of the very flexible high-level-trigger (HLT) framework of CMS, which allows to apply selections on such observables as invariant mass, decay length, transverse momentum, and rapidity, already at the trigger level. This is needed in order to keep a high trigger efficiency, coping at the same time with the strict bandwidth limitations at the HLT.

The offline selections further refine the quality of the objects used in the analyses. In particular, for the muons, the analyses described below use a set of "tight" selections, having a rate of hadrons misidentified as muons of O(0.1%) and an efficiency > 80%.

This article is structured as follows: in Section **2** we present the inclusive measurements of b hadron properties, in Section **3** we show some recent results on the reconstruction of exclusive B-hadron final states, and in Section **4** we review the measurements of charmonium properties.

2. – Inclusive b and b$\overline{\text{b}}$ Production

2˙1. *Inclusive* b *Cross Section Measurements*. – The cross section for the inclusive production of b-jets has been measured in 2010 data with two different methods: a jet-based analysis, which uses a sample corresponding to an integrated luminosity of $34\,\text{pb}^{-1}$, and a muon-based analysis, which uses a sample of $3\,\text{pb}^{-1}$ of integrated luminosity [2]. The jet data were collected using a combination of minimum-bias and single-jet triggers, while the events used in the muon analysis were required to pass a single-muon trigger, with $p_{\text{T}}^{\mu} > 9\,\text{GeV}$ and $|\eta^{\mu}| < 2.4$.

For both analyses, the b-tagging technique based on the presence of a secondary vertex is used to enhance the b fraction of the sample. In the jet analysis, the b-tagging purity is estimated with a template fit on the distribution of the secondary vertex mass, and for the muon-based one, a fit on the muon momentum transverse to the direction of the jet, $p_{\text{T}}^{\text{rel}}$, is used to discriminate between the b events and the background.

For both analyses, the main sources of systematic uncertainties are the jet energy corrections (JEC), the determination of the b-tagging efficiency and purity, and the integrated luminosity measurement.

In the left pane of Fig. 1, the measured b-jet cross section is shown as a function of the jet p_{T} for different rapidity bins. The theoretical prediction from MC@NLO [3, 4] is also shown in the figure by the solid lines. In the right pane of Fig. 1, the ratio between the measured cross section and the theoretical predictions is shown. The MC@NLO predictions are below data in the central region, and tend to be above data in the forward region.

The results of the muon-based analysis are shown in Fig. 2 as a function of the b-jet p_{T} (left) and $|y|$ (right), compared with the predictions from PYTHIA [5] and MC@NLO. The differential cross-section as a function of p_{T} is in good agreement with MC@NLO, while PYTHIA predicts higher values at low transverse momentum. The shape of the rapidity dependence measured in data is in agreement with the PYTHIA prediction, while a significant difference is observed with respect to MC@NLO.

The ratio between the b-jet and the inclusive jet cross sections is shown in the left pane of Fig. 3. The fraction of b-jets increases with p_{T} by a factor of 2, especially in the central region.

The right pane of Fig. 3 shows the results for the muon-based and the jet-based analyses of CMS, compared with two sets of measurements from the ATLAS collaboration [6]. The CMS and ATLAS results are compatible with each other, within the experimental uncertainties.

2˙2. *Inclusive* b$\overline{\text{b}}$ *Cross Section with Muon Pairs*. – The cross section for the inclusive production of b$\overline{\text{b}}$ pairs, both decaying into muons, has also been measured with $27.9\,\text{pb}^{-1}$ of data collected by CMS in 2010 [7].

The process $\text{pp} \rightarrow \text{b}\overline{\text{b}}\text{X} \rightarrow \mu\mu\text{X}'$ has been studied by looking at events containing pairs of muons, each with transverse momentum $p_{\text{T}} > 4\,\text{GeV}$ ($6\,\text{GeV}$) and pseudorapidity $|\eta| < 2.1$. The sample composition has been determined by using a two-dimensional template fit on the transverse impact parameters d_{xy} of the two muons. Templates for muons coming from b-hadron decays (B), c-hadron decays (C), and in-flight decays of pions and kaons (D) have been determined from the simulation, while the template for the prompt muon production (P) has been found from $\Upsilon \rightarrow \mu\mu$ decays in data.

Projections of the two-dimensional fits are shown in Fig. 4 for the two p_{T} thresholds studied. The fraction of events with both muons coming from B decays is $66.8 \pm 0.3\%$ for $p_{\text{T}} > 4\,\text{GeV}$ and $70.2 \pm 0.3\%$ for $p_{\text{T}} > 6\,\text{GeV}$, where the errors are statistical only.
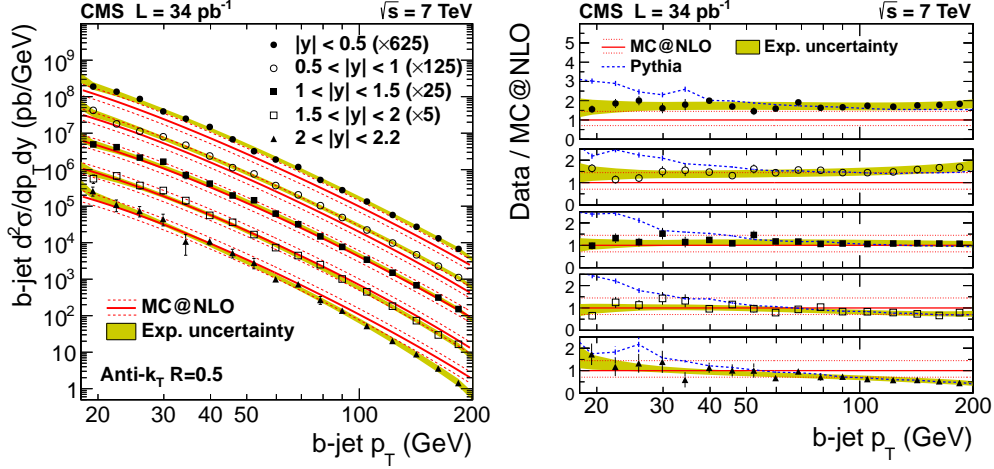
Fig. 1. – The inclusive b-jet cross section as a function of the b-jet p_T for several rapidity ranges, measured with the jet-based analysis in [2], compared with the predictions of MC@NLO (left), and the ratio between data and NLO prepdictions (right).

The main systematic uncertainties of the measurement come from the efficiency determination, from the models used to build the templates, and from the impact parameter resolution.

The measured cross sections are:

$$\sigma \left(\mathrm{pp} \to \mathrm{b\bar{b}X} \to \mu\mu\mathrm{X'}, p_T > 4\,\mathrm{GeV} \right) = 26.4 \pm 0.1(\mathrm{stat.}) \pm 2.4(\mathrm{syst.}) \pm 1.1(\mathrm{lumi.})\,\mathrm{nb},$$
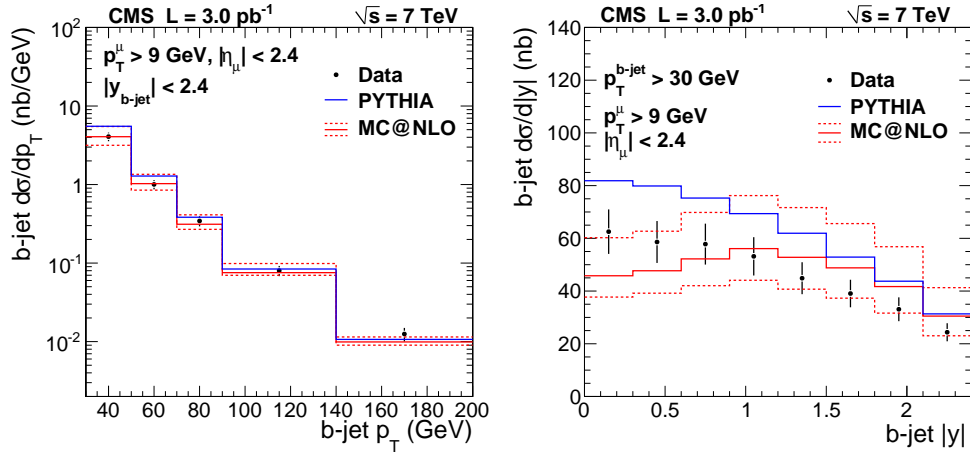

Fig. 2. – The inclusive b-jet cross section as a function of the b-jet p_T (left) and $|y|$ (right), measured with the muon-based analysis in [2], compared with the predictions of PYTHIA and MC@NLO.
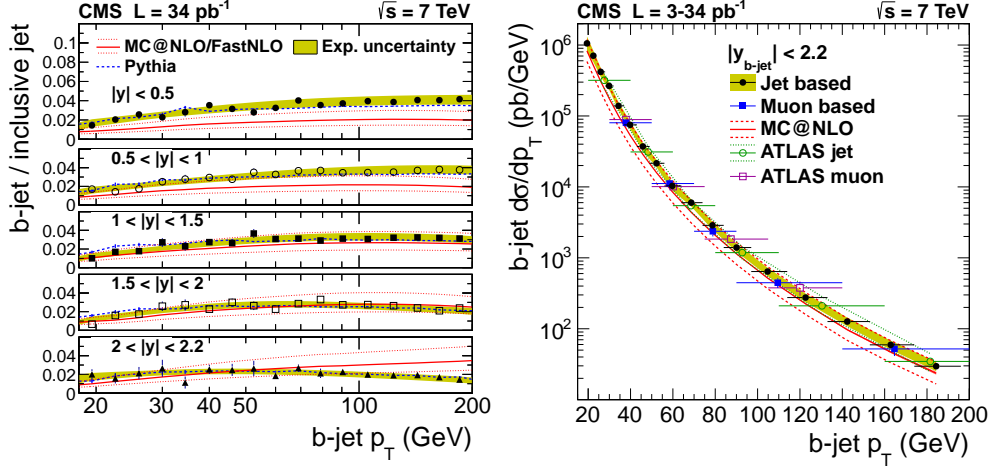
Fig. 3. – The ratio between b-jet and and the inclusive jet cross sections (left), and the comparison between the b-jet p_T spectrum for several CMS and ATLAS measurements (right) [2].

and

$$\sigma\left(\text{pp} \to \text{b}\overline{\text{b}}\text{X} \to \mu\mu\text{X}', p_T > 6\,\text{GeV}\right) = 5.12 \pm 0.03(\text{stat.}) \pm 0.48(\text{syst.}) \pm 0.20(\text{lumi.})\,\text{nb.}$$

These values can be compared with the NLO predictions from MC@NLO, that are:

$$\sigma_{\text{MC@NLO}}\left(\text{pp} \to \text{b}\overline{\text{b}}\text{X} \to \mu\mu\text{X}', p_T > 4\,\text{GeV}\right) = 19.7 \pm 0.3(\text{stat.})^{+6.5}_{-4.1}(\text{syst.})\,\text{nb},$$

and

$$\sigma_{\text{MC@NLO}}\left(\text{pp} \to \text{b}\overline{\text{b}}\text{X} \to \mu\mu\text{X}', p_T > 6\,\text{GeV}\right) = 4.40 \pm 0.14(\text{stat.})^{+1.10}_{-0.84}(\text{syst.})\,\text{nb.}$$

Both predictions are lower than the measurements, but compatible with them within the experimental and the theoretical uncertainties.

3. – Exclusive B Decays

3˙1. $\Lambda_b \to \text{J}/\psi\Lambda$ *Cross Section*. – The production cross section of the Λ_b baryon has been studied at CMS as a function of the transverse momentum and rapidity, using a data sample collected in 2011 and corresponding to an integrated luminosity of $1.9\,\text{fb}^{-1}$. The decay $\Lambda_b \to \text{J}/\psi\Lambda$, followed by $\text{J}/\psi \to \mu^+\mu^-$ and $\Lambda \to \text{p}\pi$ has been used [8].

Events are triggered by the presence of a pair of muons compatible with the decay of a J/ψ displaced by at least three standard deviations from the average position of the main proton-proton collision. Muons are selected offline by requiring them to be fully reconstructed in the tracker and in the muon stations, with "tight" quality selections.

The Λ candidates are formed from tracks with opposite charge which come from a common vertex. Candidate pairs of tracks are retained for the analysis only if they have an invariant mass compatible with the world-average Λ mass. Λ_b candidates are built by combining a J/ψ candidate and a Λ candidate coming from a common vertex, using a fit having the masses of the two particles constrained to their world-average values.
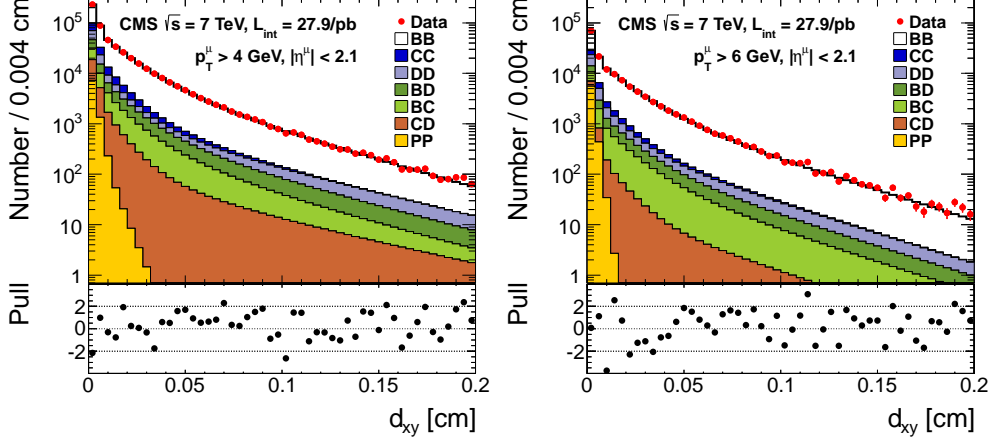
Fig. 4. – Projections of the two-dimensional template fits used to measure the cross section of the process pp → b$\bar{\text{b}}$X → $\mu\mu$X′, for $p_T > 4$ GeV (left) and $p_T > 6$ GeV (right) [7].

The overall efficiency to reconstruct the Λ_b decay chain is factorized as the product of several terms, including the efficiencies to trigger and reconstruct the single muons, and to combine them into the Λ_b candidate. The single-muon terms are taken from the data, using the Tag&Probe technique, while the simulation truth is used to estimate the effect of the di-muon correlation and to find the acceptance.

The measured differential cross sections times the branching fraction, calculated in bins of p_T and y of the Λ_b, is shown in Fig. 5 compared with the NLO predictions of POWHEG [9, 10] and with the results of PYTHIA. The slope of transverse momentum spectrum is steeper than the theoretical predictions, while the shape of the rapidity spectrum is in agreement with them, within the uncertainties.

The total cross section for $p_T^{\Lambda_b} > 10$ GeV and $\left| y^{\Lambda_b} \right| < 2.0$, obtained as the sum of all bins, is:

$$\sigma\left(\text{pp} \to \Lambda_b \text{X}\right) \times \mathcal{B}\left(\Lambda_b \to \text{J}/\psi\Lambda\right) = 1.16 \pm 0.06 \pm 0.12\,\text{nb}.$$

This is in good agreement with PYTHIA, which predicts a cross section of 1.19 ± 0.64 nb, and higher than POWHEG, which predicts $0.63^{+0.41}_{-0.37}$ nb, with uncertainties dominated by the one on $\mathcal{B}\left(\Lambda_b \to \text{J}/\psi\Lambda\right)$.

The analysis also found the ratio $\sigma\left(\overline{\Lambda}_b\right) / \sigma\left(\Lambda_b\right)$ in bins of $p_T^{\Lambda_b}$ and $\left| y^{\Lambda_b} \right|$, to be consistent with unity within the experimental precision, conferming the theoretical predictions.

3˙2. *Summary of Cross Section Measurements with Exclusive* B *Decays*. – The result for Λ_b can be compared to the previous CMS measurements of the production cross section of B^+ [11], $\bar{\text{B}}^0$ [12], and B_s [13]. Figure 6 shows the differential cross sections vs. p_T for the four particles, fitted to the Tsallis function [14]. The fit indicates a more steeply falling p_T spectrum for Λ_b than for the mesons, hinting to a change of the production rate of Λ_b relative to mesons with p_T. The observed behavior is compatible with previous measurements performed at the Tevatron [15], and with a recent result released by the LHCb collaboration [16].
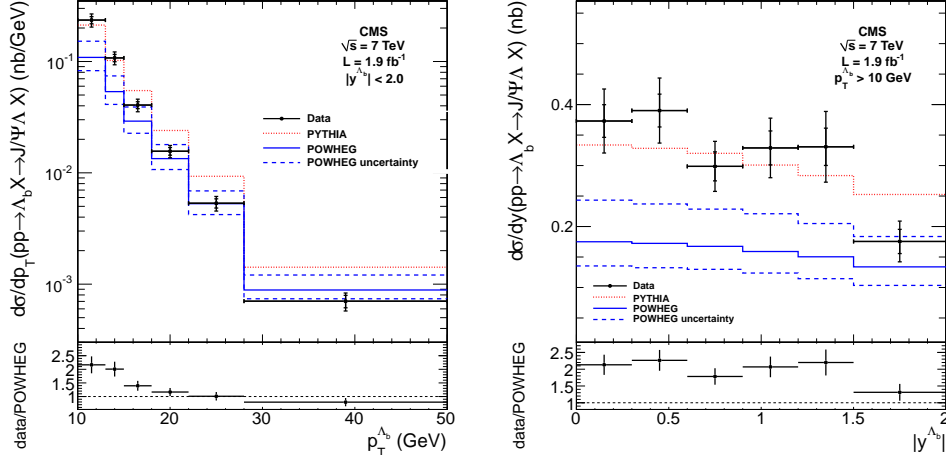
Fig. 5. – The differential cross section for the process pp $\to \Lambda_b \to J/\psi\Lambda$ as a function of the transverse momentum p_T (left) and of the rapidity y (right) of the Λ_b [8].

4. – Measurement of Charmonium Properties

The production of prompt and non-prompt J/ψ and $\psi(2s)$ has been studied on a data sample collected in 2010 by CMS and corresponding to $37\,\text{pb}^{-1}$ of integrated luminosity [17]. The decays of J/ψ and $\psi(2s)$ into $\mu^+\mu^-$ are reconstructed by looking at events triggered by the presence of two muons, and selecting pairs of muons with opposite charge which pass the "tight" quality selections and whose inner tracks come from a common vertex.

The data has been divided in bins of rapidity and transverse momentum of the J/ψ and $\psi(2s)$, and for each bin the yield of prompt and non prompt production has been found
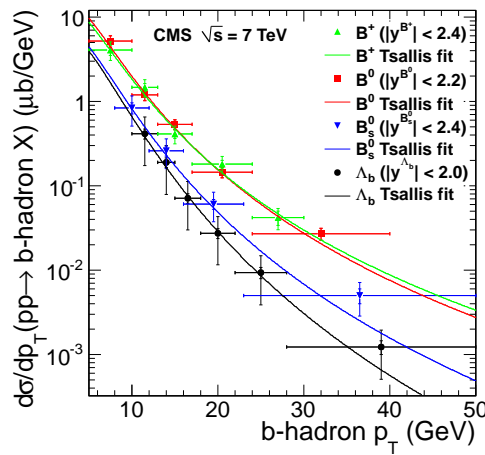

Fig. 6. – The differential cross sections as a function of the transverse momentum p_T for the four B hadrons studied at CMS [8].

with a 2D unbinned maximum-likelihood fit on the invariant mass and the *pseudo-proper decay length* ℓ of the two mesons, defined as the most probable value of the transverse distance between the di-muon vertex and the primary vertex, corrected for the Lorentz boost. The cross section in each bin is extracted from the result of the fit, corrected for the loss in efficiency and for the acceptance. The main sources of uncertainties are the statistical error of the likelihood fits, the correlations of the muon efficiencies, the vertex assignment, the models used in the fits, and the luminosity measurement.

The results for the measured cross sections are shown in Fig. 7, compared with the theoretical predictions from FONLL [18, 19]. The differential cross sections for the prompt production are in good agreement with the theory for both particles. For the non-prompt production, the cross section of the J/ψ is in agreement with the theory only for $p_T < 30\,\text{GeV}$ and is below it for larger transverse momenta, and the one of the $\psi(2s)$ is systematically lower than the prediction.

From the ratio of the non-prompt J/ψ and $\psi(2s)$ cross sections it is possible to extract the branching fraction for the processes $B \to \psi(2s) + X$. This is found to be:

$$\text{BF}\,[B \to \psi(2s) + X] = [3.08 \pm 0.12(\text{stat} - \text{syst}) \pm 0.13(\text{theor}) \pm 0.42(\text{BF}_{\text{PDG}})] \cdot 10^{-3}.$$

This value is about three times more accurate than the previous world average [20].

5. – Conclusions

In the past two years, the CMS experiment has carried out a rich program of heavy flavor physics. The inclusive cross sections for b quark production and for the production of $b\bar{b}$ pairs decaying into muons have been measured using a variety of techniques ranging from the b-tagging to the use of template fits based on p_T^{rel} and impact parameter. The cross section of the process $\Lambda_b \to J/\psi\Lambda$ has also been measured, and compared with the results previously obtained for B^0, B^+, and B_s, finding differences in the p_T behavior that hint to a dependence of the b fragmentation on the transverse momentum. Lastly, the cross section for the prompt and non-prompt production of J/ψ and $\psi(2s)$ have been measured, and from the latter, the most accurate measurement done so far of the branching ratio of $B \to \psi(2s) + X$ has been extracted.

REFERENCES

[1] CMS COLLABORATION, *JINST*, **3** (2008) S08004.
[2] CMS COLLABORATION, *JHEP*, **04** (2012) 084.
[3] FRIXIONE S. and WEBBER B. R., *JHEP*, **06** (2002) 029.
[4] FRIXIONE S., NASON P., and WEBBER B. R., *JHEP*, **08** (2003) 007.
[5] SJÖSTRAND T., MRENNA S., and SKANDS P., *JHEP*, **05** (2006) 026.
[6] ATLAS COLLABORATION, *Eur. Phys. J. C*, **71** (2011) 1846.
[7] CMS COLLABORATION, arXiv:1203.3458 [hep-ex], submitted to *JHEP*, (2012) .
[8] CMS COLLABORATION, arXiv:1205.0594 [hep-ex], submitted to *Phys. Lett. B*, (2012) .
[9] ALIOLI S., NASON P., OLEARI C., ET AL., *JHEP*, **06** (2010) 043.
[10] FRIXIONE S., NASON P., and RIDOLFI G., *JHEP*, **09** (2007) 126.
[11] CMS COLLABORATION, *Phys. Rev. Lett.*, **106** (2011) 112001.
[12] CMS COLLABORATION, *Phys. Rev. Lett.*, **106** (2011) 252001.
[13] CMS COLLABORATION, *Phys. Rev. D*, **84** (2011) 052008.
[14] TSALLIS C., *J. Stat. Phys.*, **52** (1988) 479.
[15] CDF COLLABORATION, *Phys. Rev. D*, **77** (2008) 072003.

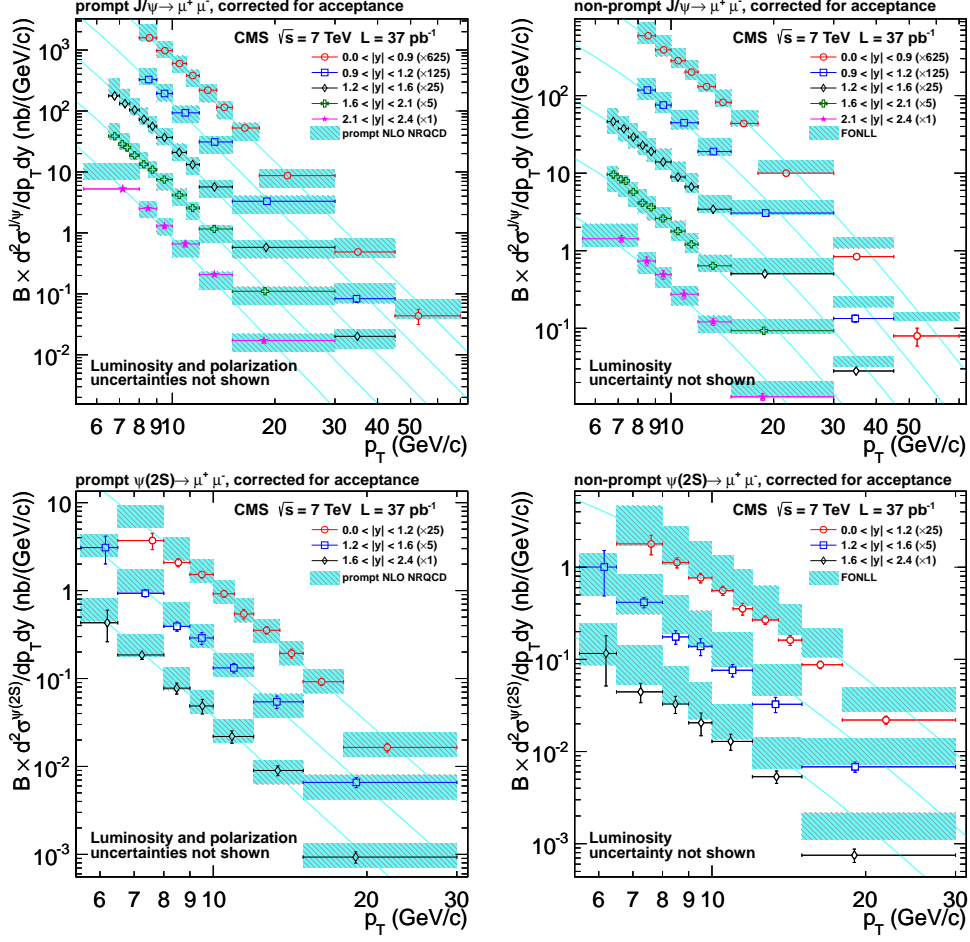Fig. 7. – Differential cross sections for the production of J/ψ (top) and ψ(2s) (bottom) as a function of the transverse momentum p_T in different rapidity ranges. Prompt production is shown in the left plots, and non-prompt in the right ones [17].

[16] LHCb Collaboration, *Phys. Rev. D*, **85** (2012) 032008.
[17] CMS Collaboration, *JHEP*, **02** (2012) 011.
[18] Cacciari M., Greco M., and Nason P., *JHEP*, **05** (1998) 007.
[19] Cacciari M., Frixione S., and Nason P., *JHEP*, **03** (2001) 006.
[20] Particle Data Group Collaboration, *J. Phys. G*, **37** (2010) 075021.